Available online at www.sciencedirect.com

SCIENCE DIRECT®

Journal of Molecular Catalysis A: Chemical 203 (2003) 277–286

JOURNAL OF MOLECULAR CATALYSIS A: CHEMICAL

www.elsevier.com/locate/molcata

Acetone transformation over PtSn/H[Al]ZSM5 catalysts

Ricardo Morales [a,b], Luis Melo [b,*], Joaquín Brito [c], Aura Llanos [d], Delfín Moronta [e], Luis Albornoz [c], Eloy Rodríguez [a]

[a] *Departamento de Química, USB, Caracas, Venezuela*
[b] *Facultad de Ingeniería, Univ. Central de Venezuela (UCV), P.O. Box 48.057, Caracas 1041-A, Venezuela*
[c] *Centro de Química, IVIC, Caracas, Venezuela*
[d] *Departamento de Química, IUT Región Capital, Caracas, Venezuela*
[e] *Facultad de Ciencias, UCV, Caracas, Venezuela*

Received 27 January 2003; received in revised form 10 April 2003; accepted 10 April 2003

Abstract

A study was carried out on the reaction of acetone transformation over bifunctional monometallic (Pt/H[Al]ZSM5, Sn/H[Al]ZSM5) and bimetallic (PtSn/H[Al]ZSM5) catalysts with variation of their tin atomic fraction (X_{Sn} = number of Sn moles/number of Sn moles + number of Pt moles). The solids prepared were analyzed by means of X-ray diffraction (XRD), nitrogen adsorption at −196 °C, chemical analysis through inductive coupled plasma–atomic emission spectroscopy (ICP–AES) technique, energy dispersive X-ray (EDX), X-ray photoelectron spectroscopy (XPS), electronic paramagnetic resonance (EPR), transmission electronic microscopy (TEM), and by means of test reaction of toluene hydrogenation. Acetone transformation was carried out at 160 °C, under atmosphere pressure, at an acetone/hydrogen molar ratio of 3 and varying WHSV. The results obtained show a sensitive variation in the catalytic properties as X_{Sn} is varied in the series of PtSn/H[Al]ZSM5 catalysts prepared; these changes are attributed to the presence of effects of the electronic and geometric type, which would be a consequence of the formation of a Pt–Sn alloy and probably of the phenomenon of decoration of platinum particles, which is evidenced from the evaluation of the solids by means of XPS and EPR.

Keywords: Acetone; Methyl isobutyl ketone; PtSn/H[Al]ZSM5; Bifunctional monometallic and bimetallic catalysts

1. Introduction

The selective hydrogenation of organic molecules with different functional groups capable of being hydrogenated is one of the main goals in processes of fine chemical synthesis [1]. Recent studies show that medium-pore zeolites are capable of transforming acetone into 4-methyl-3-penten-2-one (known as mesityl oxide (MO)) [2,3]. This α-β-insaturated ketone is the closest intermediary in the synthesis of 4-methyl-2-pentanone, known as methyl isobutyl ketone (MIBK), which is a substance widely used in the manufacturing of a great deal of products, such as dies, lacquers, painting, varnishes and as a solvent for nitrocellulose, ethylcellulose, and natural and synthetic resins [4].

MIBK has been synthesized by means of a process involving numerous stages. The first one consists of the aldolization of two acetone molecules (1) to obtain 4-hydroxi-4-methyl-2-pentanone or diacetone alcohol (DA). This stage is usually catalyzed by acids and mineral bases. The second stage is DA dehydration, which is normally carried out through acid catalysis, using

* Corresponding author.
E-mail address: melol@camelot.rect.ucv.ve (L. Melo).

1381-1169/03/$ – see front matter © 2003 Elsevier B.V. All rights reserved.
doi:10.1016/S1381-1169(03)00367-4

H_3PO_4 or H_2SO_4 (2) to obtain MO. The last stage is the selective hydrogenation of the MO olefinic double bond (C=C) to obtain MIBK (3), which consists of a process carried out over a supported metallic stage [5]:

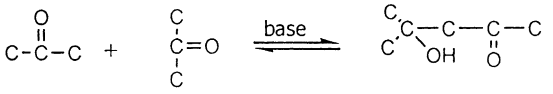

(1)

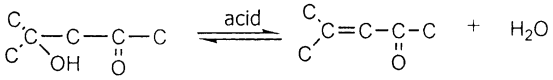

(2)

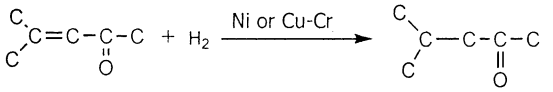

(3)

However, this complex process has been recently studied in a single apparent stage, under hydrogen atmosphere and using bifunctional catalysts with metals (Pt, Pd, Ni, . . .), supported over acid and basic solids and crystalline aluminosilicates [6–8].

Over the last decade, bimetallic catalysts have been found to have a wide application in selective hydrogenation processes. These solids show numerous advantages over catalysts with a single metal, because they are certainly more selective and stable, and, therefore, find wide applications in reactions of fine chemical synthesis. The effects of a second metallic component are very specific and depend, among other factors, both on the nature of the metals dispersed over the support surface as well as on the atomic radii of the metals used and, of course, on the type of reaction studied [9]. Different research groups have found that the addition of promoters, such as Sn, over Pt catalysts improve their catalytic capability for hydrogenation–dehydrogenation reactions [10]. The formation of an alloy between Pt and Sn could explain the improvement of the properties of these catalysts, which could reduce the size of the Pt agglomerates, thus resulting in lower coke formation and higher selectivity [11].

In this sense, this work is aimed at studying the reaction of acetone transformation over bifunctional monometallic catalysts (Pt/H[Al]ZSM5 and Sn/H[Al]ZSM5) as well as over bifunctional bimetallic catalysts (PtSn/H[Al]ZSM5) with a view to assess how is the catalytic behavior of solids when their tin atomic fraction (X_{Sn}) is varied.

2. Experimental

An aluminosilicate of the MFI type was synthesized using the method proposed by Guth and Caullet [12]. The solid obtained was calcined at 550 °C in the presence of air to eliminate the orienting agent and then was exchanged with a 1 M $NH_4(CH_3COO)$ solution. Once the solid is exchanged, it is dried and calcined again in the presence of dry air at 550 °C for 6 h. The synthesized zeolite was characterized by means of X-ray diffraction (XRD), nitrogen adsorption at −196 °C, chemical analysis by means of the inductive coupled plasma–atomic emission spectroscopy (ICP–AES) technique and energy dispersive X-ray (EDX) analysis.

The synthesized aluminosilicate was used as a support in the preparation of the bifunctional catalysts, by means of the simultaneous exchange–impregnation method, which made it possible to introduce the desired amounts of platinum and tin, using $Pt(NH_3)_4Cl_2$ and $SnCl_2{\cdot}2H_2O$ as precursor salts. The catalysts prepared were: 0.5% Pt/H[Al]ZSM5, 1.0% Sn/H[Al]ZSM5 and 0.5% Pt-*x*% Sn/H[Al]ZSM5 (where *x* is the percentage of tin introduced). The content of the supported phase (Pt and/or Sn) was determined through the ICP–AES technique. The solids obtained were calcined for 6 h under dry air atmosphere (Pt/H[Al]ZSM5 at 300 °C [13] and Sn/H[Al]ZSM5 and PtSn/H[Al]ZSM5 at 500 °C [14]). Then each solid was reduced at 500 °C over the same period of time, but under dry hydrogen atmosphere.

The following solids from the series of catalysts prepared were evaluated by means of X-ray photoelectron spectroscopy (XPS), electronic paramagnetic resonance (EPR) and transmission electronic microscopy (TEM): Pt/H[Al]ZSM5, Sn/H[Al]ZSM5 and PtSn/H[Al]ZSM5 (with $X_{Sn} = 0.46$). The XPS analysis was conducted in an X-ray photoelectron spectrometer (VG Scientific, ESCALAB 220i-XL model), equipped with an Al/Mg source. The reduction treatment was carried out "in situ", by heating the fresh samples under a hydrogen flow at 500 °C for 2 h, to avoid any contact with air. The spectra of the reduced catalysts were taken under vacuum of the 10^{-8} to 10^{-11} mbar order and using the signal of Si 2p at 102.9 eV [15] as a reference. Evaluation by means of EPR was carried out at room temperature using a Varian E-line, X band spectrometer with a rectangular cavity operating under TE_{102} mode.

The assessment by means of transmission electronic microscopy was made using a Phillips electronic microscope, CM-10 model, operated at 120 kV. Samples for this analysis were treated as follows: a suspension of the catalyst to be analyzed was prepared with 30% ethanol; then ultrasound was applied for 5 min and once the homogeneous suspension was obtained a drop was placed on a copper grid, which had been previously covered with collodion and coal.

On the other hand, the series of bifunctional monometallic and bimetallic catalysts prepared was analyzed by means of the toluene hydrogenation reaction under atmosphere pressure, at 110 °C, $P_{H_2}/P_{toluene} = 4$ and WHSV $= 21.5\,h^{-1}$. The acetone transformation was carried out under atmosphere pressure, at 160 °C, $P_{Ac}/P_{H_2} = 3$ and variable WHSV. The reactor effluents were in line injected into an HP-6890 chromatograph, equipped with an FID detector and a 30 m CP-sil-5CB column, so that the analysis of the different products generated could be possible.

3. Results and discussion

Once analyzed through ICP–AES, the Si/Al ratio of the synthesized aluminosilicate was found to be 15; this finding was confirmed by means of EDX, which showed a Si/Al ratio of 14.7, clearly indicating that the solid surface composition is very similar to that obtained by ICP–AES. This result suggests that this solid has a fairly homogeneous chemical composition. The specific surface area (SSA) of this solid is reported in Table 1. These results, together with those obtained from the X-ray diffraction analysis, make it possible to state that this zeolite is of the MFI type and highly pure and crystalline.

The content of the supported metallic phase of the bifunctional monometallic and bimetallic catalysts prepared using the exchange–impregnation method was analyzed to verify whether the platinum and tin concentrations in these solids were within the desired range, as can be seen in Table 1. In addition, tin atomic fraction, X_{Sn}, was determined for every catalyst, which is also reported in the same table. According to this table, the number of catalysts prepared presents X_{Sn} values distributed throughout the range within 0–1, as expected.

Table 1
Physicochemical characteristics of the series of monometallic and bimetallic bifunctional catalysts prepared

Catalysts	Pt (%) (expected)	Sn (%) (expected)	X_{Sn}	SSA (m^2/g)	AH_0 (mmol/(h g Pt))	D (%)
H[Al]ZSM5	–	–	–	380	–	–
0.50% Pt/H[Al]ZSM5[a]	0.47	–	0	375	3300	48.0
0.50% Pt-0.10% Sn/H[Al]ZSM5	0.44	0.08	0.24	372	1570	–
0.50% Pt-0.30% Sn/H[Al]ZSM5[a]	0.49	0.26	0.46	373	470	49.0
0.50% Pt-0.50% Sn/H[Al]ZSM5	0.46	0.43	0.58	374	0	–
0.50% Pt-0.70% Sn/H[Al]ZSM5	0.50	0.70	0.70	370	0	–
1.0% Sn/H[Al]ZSM5	–	0.80	1.0	375	0	–

Pt (%), Sn (%), wt.% of platinum and tin determined by means of ICP–AES. X_{Sn}: tin atomic fraction present in every catalyst; SSA: specific surface area; D (%): platinum dispersion determined by TEM; AH_0: activity in toluene hydrogenation extrapolated at zero time per gram of platinum.

[a] Catalysts assessed by means of TEM.

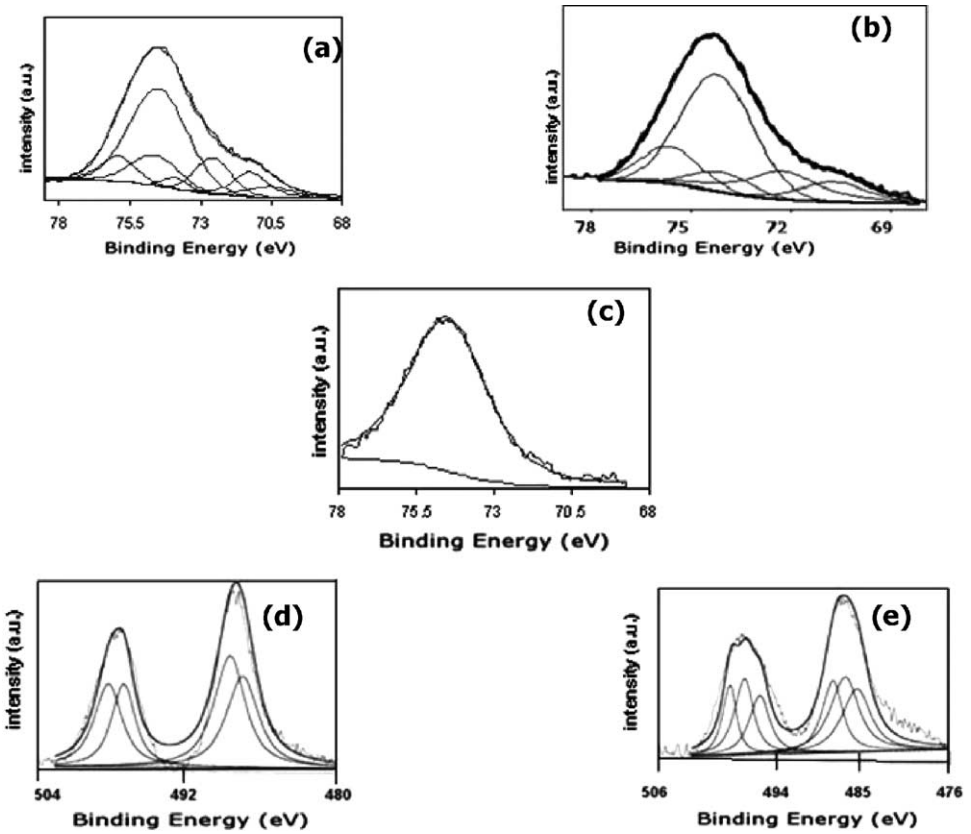

Fig. 1. XPS spectra for: (a) H[Al]ZSM5 in the Al 2p zone, (b) 0.50% Pt/H[Al]ZSM5 in the Pt 4f zone, (c) PtSn/H[Al]ZSM5 ($X_{Sn} = 0.46$) in the Pt 4f zone, (d) 1.0% Sn/H[Al]ZSM5 in the Sn 3d zone and (e) PtSn/H[Al]ZSM5 ($X_{Sn} = 0.46$) in the Sn 3d zone.

It can also be observed in Table 1 that SSA of the bifunctional catalysts ranges within 370 and 380 m^2/g, meaning that the introduction of the supported metallic phase does not block the support microporosity.

3.1. XPS analysis

The characterization through X-ray photoelectron spectroscopy was aimed at obtaining information on the oxidation states of the supported phase (Pt and/or Sn) on the surface of the solid.

The XPS spectra obtained for the support and the Pt/H[Al]ZSM5, Sn/H[Al]ZSM5 and PtSn/H[Al]ZSM5 catalysts are shown in Fig. 1. Each one of these spectra was deconvoluted, evidencing a number of signals in each one of the treated spectra. Of course, these signals should correspond to the different chemical species present on the catalyst surface. Table 2 shows

Table 2
Binding energies determined by XPS (in eV)

Catalyst	Si 2p (reference)	Al 2p	Pt $4f_{7/2}$	Sn $3d_{3/2}$
H[Al]ZSM5	102.9	74.5	–	–
Pt/H[Al]ZSM5	102.9	74.5	70.9–72.2	–
Sn/H[Al]ZSM5	102.9	74.5	–	488.6–487.6
PtSn/H[Al]ZSM5 ($X_{Sn} = 0.46$)	102.9	74.5	70.4–71.3–72.3	488.5–487.3–485.9

All BE are referred to Si 2p = 102.9.

the values of binding energy (BE) corresponding to the chemical species present in the different catalysts studied. These binding energies were referred to the signal of Si 2p = 102.9 eV, which is a reference value used for a support of the crystalline aluminosilicate type, as the one used in this work [15].

Fig. 1a shows the XPS spectrum for the support, where only one peak appears at 74.5 eV, which corresponds to Al 2p signal. According to the XPS spectrum for the Pt/H[Al]ZSM5 catalyst (Fig. 1b), the Pt $4f_{7/2}$ signal appears to be overlapped with the one corresponding to Al 2p, which undoubtedly makes it difficult to use this spectrum; however, due to the deconvolution to which the spectrum was subjected, signals could be identified at 70.9 and 72.2 eV, corresponding to the Pt^0 and PtO_{ads} species, as shown in Table 2. Similar values for these species were reported by Kim et al. [16].

Fig. 1d shows the XPS spectrum for the bifunctional Sn/H[Al]ZSM5 catalyst, where only two peaks appear at 487.6 and 488.6 eV, which correspond to oxidized tin species (Sn(II) and/or Sn(IV)). Now, since a discrimination between Sn(II) and Sn(IV) [17,18] is not possible by means of the XPS studies, in this catalyst we can only confirm the presence of tin in its oxidized form; however, it is worth highlighting that before their analysis, these samples were treated for 6 h under hydrogen atmosphere at 500 °C, showing how difficult it is to reduce this metal to Sn^0 over a support such as H[Al]ZSM5.

The presence of a strong interaction between tin and structural oxygen and/or between this metal and the aluminum in the zeolite, which could result in the formation of a bond between aluminum and tin [19], could be the reason why tin supported over the H[Al]ZSM5 zeolite cannot be completely reduced. However, these interactions do not exist when support solids such as SiO_2 or carbon black are used. When these catalysts were subjected to XPS analysis, they showed a signal at 485.3 eV, which is assigned to Sn^0 [17,18].

However, according to the XPS spectrum (Fig. 1c), the bimetallic PtSn/H[Al]ZSM5 catalyst was found to have three signals in the Pt 4f region. These signals are found at the following binding energies: 70.4, 71.3 and 72.3 eV, which could be assigned to the Pt species alloyed with Sn, Pt^0 and PtO_{ads}, respectively. This would imply that a considerable part of the reduced platinum could be receiving electronic density from tin, such as has been expressed by Stagg et al. [11]; this could be the main reason why the new Pt $4f_{7/2}$ signal is produced at lower values of binding energy (70.4 eV). Now, if the signal of the alloyed platinum moves towards lower binding energy values due to the effect of the admission of the charge density, a similar but opposite phenomenon should occur for the signal of the alloyed tin. In this sense, when the Sn 3d region of this catalyst spectrum (Fig. 1e) is analyzed, three peaks are clearly observed, located at 485.9, 487.3 and 488.5 eV; these signals correspond to species of reduced (Sn^0) and oxidized (Sn(II) and/or Sn(IV)) tin. It can be observed that the signal attributable to Sn^0 is somehow displaced towards higher binding energies with respect to the one reported by Coloma et al. [17,18]; this displacement suggests that this metal would be giving up electronic density. We think that this phenomenon would be occurring from tin towards platinum, which would mean that both metals represent a Pt–Sn alloy. This type of alloy has been reported by Kappenstein et al. [20] and Lieske and Völter [21] in their studies of $PtSn/Al_2O_3$ catalysts.

3.2. Electronic paramagnetic resonance (EPR) analysis

To confirm the previous results we have assessed the catalysts mentioned before by means of electronic paramagnetic resonance spectroscopy. The spectra obtained for the support as well as for the different bifunctional monometallic and bimetallic catalysts used are reported in Fig. 2 (H[Al]ZSM5 (a), Pt/H[Al]ZSM5 (b), Sn/H[Al]ZSM5 (c) and PtSn/H[Al]ZSM5 (X_{Sn} = 0.46) (d)). It is worth mentioning that all EPR spectra will be represented with a 5×10^4 gain for comparative purposes.

Fig. 2a shows the EPR spectrum for an aluminosilicate of the MFI type used as a support in all of the catalysts prepared, once it was calcined under air stream and reduced under hydrogen atmosphere; no signal of paramagnetism is observed. However, Fig. 2b presents the spectrum of the calcined and reduced bifunctional Pt/H[Al]ZSM5 catalyst with a paramagnetic signal (g = 2.04), which would be indicative of the existence of different magnetic environments between H[Al]ZSM5 and Pt/H[Al]ZSM5, thus suggesting that the species detected by XPS on

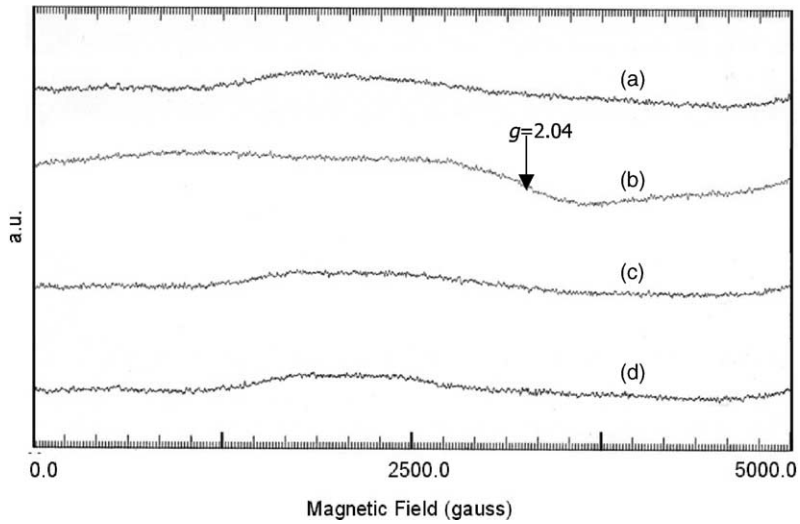

Fig. 2. EPR spectra for: (a) support, (b) 0.50% Pt/H[Al]ZSM5, (c) 1.0% Sn/H[Al]ZSM5 and (d) PtSn/H[Al]ZSM5 ($X_{Sn} = 0.46$).

this catalyst surface (Pt^0 and/or PtO_{ads}) would be responsible for the presence of unpaired electrons in this solid. Notwithstanding, since the PtO species could be diamagnetic, we should then consider that Pt^0 represents the species giving rise to the paramagnetism detected in the Pt/H[Al]ZSM5 catalyst.

The bifunctional Sn/H[Al]ZSM5 catalyst was also subjected to calcination and reduction processes and was finally subjected to EPR analysis. Its spectrum is presented in Fig. 2c, showing no paramagnetic signals. This undoubtedly suggests that the tin species on the solid surface (oxides (II and/or IV) as shown through XPS) does not possess any magnetic environment implying the existence of unmatched electrons in its orbitals.

Fig. 2d shows the spectrum of the bifunctional bimetallic PtSn/H[Al]ZSM5 catalyst obtained after calcination and reduction. It can be observed that this catalyst does not present either visible signals in the EPR analysis. This means that it has a magnetic environment which suggests that there basically exist diamagnetic species on its surface, or their proportion is at least substantially higher than the paramagnetic ones. In this sense, it is evident that the results of the EPR analysis are perfectly compatible with the results obtained by means of XPS, since this technique was used to demonstrate the presence of PtO_{ads}, Pt^0, Pt–Sn and Sn in form of oxides (II and/or IV). Now, since most of the platinum and tin species detected on the catalyst surface appear to be diamagnetic, we think that the paramagnetism resulting from Pt^0 in this solid would not be detectable due to the reduced concentration of this species on the surface of the bimetallic PtSn/H[Al]ZSM5 catalyst.

3.3. Analysis based on toluene hydrogenation and TEM

Since the reaction of toluene hydrogenation is sensitive to the density of metallic centers accessible to the reactive as well as to the nature of the supported phase [7], we have used this fact to correlate its hydrogenating activity per gram of platinum, extrapolated at zero time (AH_0) with the population of metallic centers present in these catalysts, and evidence possible disturbances due to the presence of effects of the electronic and/or geometric type on the supported metal particles. In this sense, according to Table 1, AH_0 is considerably affected as a result of the increase in the tin content in the catalyst, to such extent that when the PtSn/H[Al]ZSM5 ($X_{Sn} = 0.46$) solid is considered instead of the Pt/H[Al]ZSM5 ($X_{Sn} = 0.00$) one, the hydrogenating activity decreases almost seven times. This reduction in AH_0 could be attributed in principle to a decrease in platinum dispersion as a consequence of the addition of tin; however, dispersion of

the metallic phase for both catalysts was determined through TEM and it was found to be 50% for each one (Figs. 3 and 4). This means that the suppression of the hydrogenating activity shall depend on the presence of another phenomenon, which, in this case seems to be the presence of effects of the electronic and/or geometric type; but since the specific hydrogenating activity substantially decreases from the catalyst with $X_{Sn} = 0.00$ to the solid with $X_{Sn} = 0.46$ (Table 1), we consider that the phenomenon that would be acting upon these catalysts would basically be an effect of the electronic type by means of which tin gives up electronic density to platinum, as has been suggested by the analyses conducted through XPS and EPR.

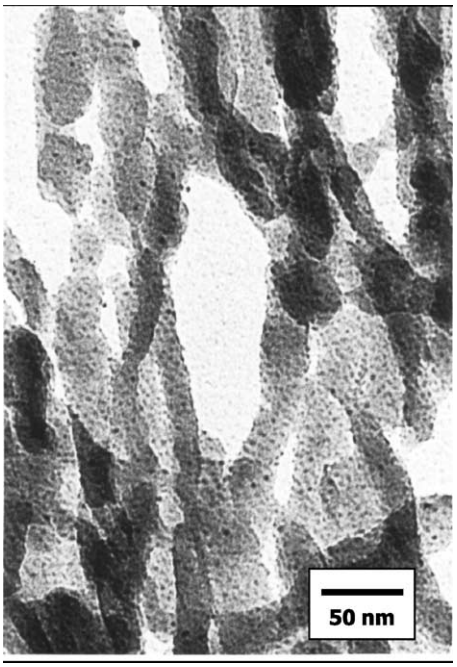

Fig. 3. TEM micrograph for the 0.50% Pt/H[Al]ZSM5 catalyst.

3.4. Acetone transformation

Acetone transformation over the different solids prepared and characterized was carried out under the previously specified conditions and at variable WHSV. Fig. 5 presents the evolution of the initial total activity (A_0) and of the starting formation rates (r_0) of the different products generated in this reaction as a function of the tin atomic fraction (X_{Sn}) in every catalyst.

According to this figure, A_0 is lower when X_{Sn} increases, with a decrease of 25% in the catalyst with $X_{Sn} = 0.00$ with respect to the solid with $X_{Sn} = 0.46$. However, it is also worth mentioning that A_0 for the catalyst with $X_{Sn} = 1.00$ decreases 80% with respect to the solid with $X_{Sn} = 0.00$; this could be explained if we consider (a) that the acetone transformation under hydrogen atmosphere and over bifunctional catalysts of the type used in this work takes place through the following reaction scheme [22]:

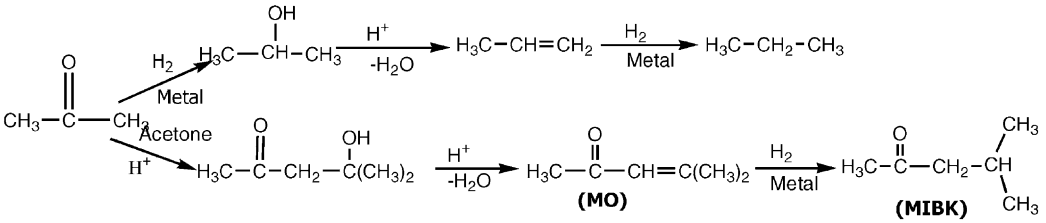

and (b) that with the increase in the tin content in the solids, its activity towards the hydrogenation reaction is lower, as demonstrated by toluene hydrogenation (Table 1). In this sense, as X_{Sn} increases over these catalysts, the hydrogenation reactions of acetone, propene, mesityl oxide, etc. will be more restricted. This phenomenon would be basically associated to the formation of the Pt–Sn alloy and/or to the presence of oxidized tin species (II and/or IV), which were detected on the surface of the catalysts by means of the XPS technique; these species are characteristic because they are little active in the hydrogenation processes.

We also believe that selectivity towards the products generated over each one of these solids, as well as their useful life, will change as a result of a variation in the nature and/or composition of the supported metallic particles.

In this sense, Fig. 5 shows the evolution of the starting formation rates of the main products of the acetone transformation. It can be clearly seen that as X_{Sn}

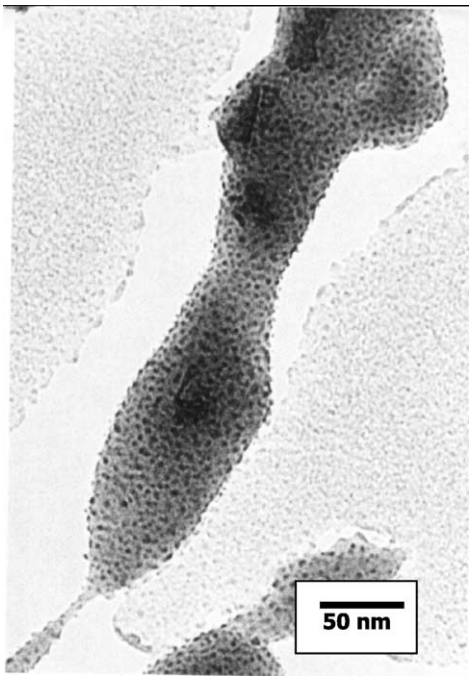

Fig. 4. TEM micrograph for the PtSn/H[Al]ZSM5 catalyst ($X_{Sn} = 0.46$).

increases the propane starting formation rate [r_0(Hc)] continuously decreases to such an extent that it goes from 83 mmol/(h g) to practically 30 mmol/(h g) from the catalyst with $X_{Sn} = 0.00$ (Pt/H[Al]ZSM5) to the solid with $X_{Sn} = 0.46$ (PtSn/H[Al]ZSM5), this drop in the r_0(Hc) values cannot be related to a decrease in the dispersion of the supported metallic phase as a result of the change from catalyst $X_{Sn} = 0.00$ to $X_{Sn} = 0.46$, since this parameter has been evaluated by TEM for both catalysts (Figs. 3 and 4). The average size of the metallic particles was found to be similar in both cases.

Therefore, these results suggest that the substantial decrease in the r_0(Hc) values would be related to the presence of effects of the electronic and/or geometric type resulting from the existence of Pt, Pt–Sn metallic centers and the Pt–Sn alloy covered by oxidized tin species. As a consequence these latter are little active in the hydrogenation of the carbonyl double bond (C=O) of acetone which is a stage required in the propane formation.

According to Fig. 5, the starting formation rate of MIBK [r_0(MIBK)], contrary to the r_0(Hc), is initially higher as X_{Sn} increases; this phenomenon occurs until a maximum is reached with the catalyst with $X_{Sn} = 0.46$; however, it can be observed that r_0(MIBK) considerably drops for all of the solids with $X_{Sn} > 0.46$. These results suggest the presence of an effect of the electronic type for the solids with X_{Sn} within the $0.00 < X_{Sn} \leq 0.46$, and of the geometric type combined with one of the electronic type for solids with $X_{Sn} > 0.46$.

In our opinion, these effects are behaving as already described, because the catalysts with $X_{Sn} \leq 0.46$ (Pt-rich catalysts) present growing selectivity towards hydrogenation of the olefinic double bond (C=C) of MO as X_{Sn} increases, which progressively decreases as

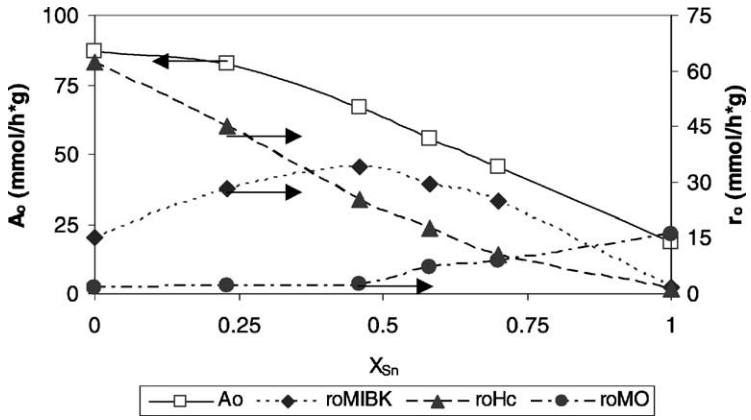

Fig. 5. Evolution of the starting global activity (A_0) and of the starting formation rate (r_0) of the main products in the acetone transformation as a function of X_{Sn} at 160 °C, 1 atm, $P_{Ac}/P_{H_2} = 3$ and WHSV = 9.4 h^{-1}.

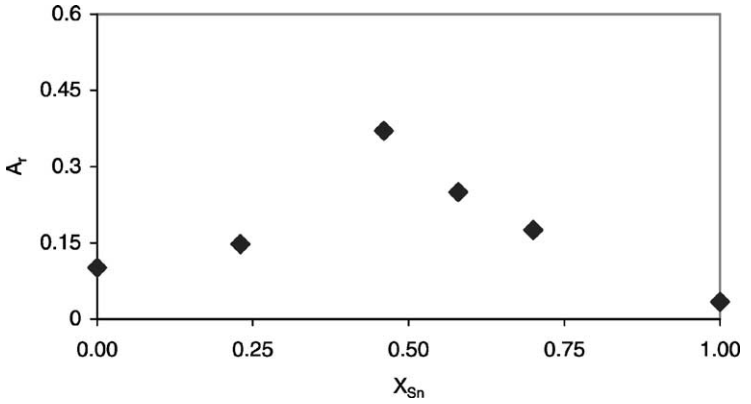

Fig. 6. Evolution of the residual activity (Ar = A_t/A_0) as a function of X_{Sn} at 160 °C, 1 atm, $P_{Ac}/P_{H_2} = 3$ and WHSV = 9.4 h^{-1}.

X_{Sn} is higher for all of the solids with $X_{Sn} > 0.46$. The results for these last catalysts suggest that the metallic particles (platinum and/or Pt–Sn alloy) could be being progressively covered by oxidized tin species (the main form in which tin is present as X_{Sn} increases).

It is also interesting to mention that since r_0(Hc) and r_0(MIBK), respectively, decrease and increase when going from the catalyst with $X_{Sn} = 0.00$ to the solid with $X_{Sn} = 0.46$, the metallic centers required for hydrogenating the acetone carbonyl double bond (C=O) (process necessary for the propane formation) are different to those required for hydrogenation of the olefinic double bond (C=C) of MO (necessary for MIBK formation) or that they are simply hydrogenation processes carried out by completely different mechanisms.

Regarding the evolution of the starting rate of mesityl oxide formation [r_0(MO)], it can be observed in Fig. 5 that r_0(MO) is practically zero for the catalysts with $X_{Sn} \leq 0.46$, which is a logical result since the metallic centers present in these solids are more selective towards the hydrogenation of the olefinic double bond of MO; however this is not the case for the catalyst with $X_{Sn} > 0.46$, which present a considerable increase in r_0(MO). These results are compatible with the lower concentration of MIBK that is generated over these solids, meaning that the catalysts with $X_{Sn} > 0.46$ behave more and more as typical monofunctional acid catalysts as X_{Sn} goes over 0.46 (Sn-rich catalysts).

In addition, we should assume that as hydrogenating activity of these solids changes, their useful life will also vary, because their stability (expressed as a function of residual activity, Ar $= A_t/A_0$) is closely related to their ability for hydrogenating the main coke precursors formed in this reaction. In this regard, Fig. 6 presents the evolution of the catalysts stability (Ar) as X_{Sn} is increased. It can be clearly observed that Ar goes to a peak, which is reached with the catalyst with the higher MO hydrogenation capability, that is, with the solid with $X_{Sn} = 0.46$, which confirms that MO is the main precursor of the oxygenated coke that deactivates these catalysts [7].

4. Conclusions

The results obtained express that the increase in the tin atomic fraction (X_{Sn}) in the PtSn/H[Al]ZSM5 catalysts has a significant effect upon the catalytic properties of the solids (activity, selectivity and stability), which has been attributed to the presence of some phenomena basically of the electronic type for all of the catalysts with $X_{Sn} \leq 0.46$, and of the electronic type combined with a geometric one for all of the catalysts with $X_{Sn} > 0.46$. The product of interest in the reaction of acetone transformation, methyl isobutyl ketone, is preferentially formed over the PtSn/H[Al]ZSM5 catalysts, with $X_{Sn} \sim 0.50$. The highest selective hydrogenation of the olefinic double bond of mesityl oxide for MIBK formation is observed in the catalysts with $X_{Sn} \sim 0.50$.

References

[1] P. Fouilloux, in: M. Guisnet, et al. (Eds.), Heterogeneous Catalysis and Fine Chemicals I, Elsevier, Amsterdam, 1988, p. 123.
[2] L. Melo, Ph.D. Thesis, Université de Poitiers, France, 1994.
[3] A.I. Biaglow, J. Sepa, R.J. Gorte, D. White, J. Catal. 151 (1995) 373.
[4] W. Hoelderich, Stud. Surf. Sci. Catal. 41 (1988) 83.
[5] W. Reith, M. Dettmer, H. Widdecke, B. Flischer, Stud. Surf. Sci. Catal. 59 (1991) 487.
[6] P.V. Chen, S.J. Chu, N.S. Chang, T.J. Chuang, L.Y. Chen, Stud. Surf. Sci. Catal. 46 (1984) 83.
[7] L. Melo, G. Giannetto, F. Alvarez, P. Magnoux, M. Guisnet, Catal. Lett. 44 (1997) 201.
[8] D. Goñi, L. Melo, G. Gianneto, P. Magnoux, M. Guisnet, N. Lavaud, in: Proceedings of the XVII Simposio Iberoamericano de Catálisis, vol. I, 2000, p. 413.
[9] A. Palazov, Ch. Bonev, D. Shopov, G. Lietz, A. Sárkány, J. Völter, J. Catal. 103 (1987) 249.
[10] C. Audo, J.F. Lambert, M. Che, B. Didillon, Catal. Today 65 (2001) 157–162.
[11] S.M. Stagg, C.A. Querini, W.E. Alvarez, D.E. Resasco, J. Catal. 168 (1997) 75.
[12] J.L. Guth, Ph. Caullet, J. Chim. Phys. 83 (1986) 155.
[13] G. Giannetto, G. Perot, M. Guisnet, Stud. Surf. Sci. Catal. 20 (1985) 265.
[14] C. Larese, J.M. Campos-Martín, J.A. Delgado, J.L.G. Fierro, in: Proceedings of the XVII Simposio Iberoamericano de Catálisis, vol. I, 2000, p. 129.
[15] T.L. Barr, Recent advances in X-ray photoelectron spectroscopy studies of oxides, J. Vac. Sci. Technol. A 9 (3) (1991) 1793–1805.
[16] K.S. Kim, N. Winograd, R.E. Davis, J. Am. Chem. Soc. 93 (1971) 6296.
[17] F. Coloma, A. Sepúlveda-Escribano, J.L.G. Fierro, F. Rodríguez-Reinoso, Appl. Catal. A: Gen. 148 (1996) 63.
[18] F. Coloma, A. Sepúlveda-Escribano, J.L.G. Fierro, F. Rodríguez-Reinoso, Appl. Catal. A: Gen. 136 (1996) 231.
[19] K. Balakrishnan, Y.J. Schwank, J. Catal. 127 (1991) 287–306.
[20] C. Kappenstein, M. Guérin, K. Lázár, K. Matusek, Z. Paál, J. Chem. Soc., Faraday Trans. 94 (1998) 2463.
[21] H. Lieske, J. Völter, J. Catal. 90 (1984) 96.
[22] L. Melo, P. Magnoux, G. Giannetto, F. Alvarez, M. Guisnet, J. Mol. Catal. A: Chem. 124 (1997) 155.